HHS Public Access

Author manuscript

Proc SPIE Int Soc Opt Eng. Author manuscript; available in PMC 2019 March 01.

Published in final edited form as:

Proc SPIE Int Soc Opt Eng. 2018 March ; 10578: . doi:10.1117/12.2293685.

A Structural Connectivity Approach to Validate a Model-based Technique for the Segmentation of the Pulvinar Complex

Srijata Chakravorti[a], **Victoria L. Morgan**[b], **Paula Trujillo-Diaz**[c], **Raul Wirz**[a], and **Benoit M. Dawant**[a]

[a]Department of Electrical Engineering and Computer Science, Vanderbilt University, Nashville, TN, USA

[b]Department of Radiology and Radiological Sciences, Vanderbilt University Institute of Imaging Science, Vanderbilt University Medical Center, Nashville, TN, USA

[c]Department of Neurology, Vanderbilt University Medical Center, Nashville, TN, USA

Abstract

The pulvinar of the thalamus is a higher-order thalamic nucleus that is responsible for gating information flow to the cortical regions of the brain. It is involved in several cortico-thalamocortical relay circuits and is known to be affected in a number of neurological disorders. Segmenting the pulvinar in clinically acquired images is important to support studies exploring its role in brain function. In recent years, we have proposed an active shape model method to segment multiple thalamic nuclei, including the pulvinar. The model was created by manual delineation of high resolution 7T images and the process was guided by the Morel stereotactic atlas. However, this model is based on a small library of healthy subjects, and it is important to validate the reliability of the segmentation method on a larger population of clinically acquired images. The pulvinar is known to have particularly strong white matter connections to the hippocampus, which allows us to identify the pulvinar from thalamic regions of high hippocampal structural connectivity. In this study, we obtained T1-weighted and diffusion MR data from 43 healthy volunteers using a clinical 3T MRI scanner. We applied the segmentation method to the T1-weighted images to obtain the intrathalamic nuclei, and we calculated the connectivity maps between the hippocampus and thalamus using the diffusion images. Our results show that the shape model segmentation consistently localizes the pulvinar in the region with the highest hippocampal connectivity. The proposed method can be extended to other nuclei to further validate our segmentation method.

Keywords

Thalamic nuclei segmentation; pulvinar; MRI; DTI; probabilistic tractography

Further author information: (Send correspondence to Srijata Chakravorti), Srijata Chakravorti: srijata.chakravorti@vanderbilt.edu.

1. INTRODUCTION

The thalamus is a structure located in the deep brain right above the brain stem that is responsible for modulating the flow of information from the cerebral cortex to the basal ganglia and back. It is involved in a wide range of functions including motor, sensory, integrative and higher order cortical functions. It is structurally and functionally diverse, and can be subdivided into neuronal clusters known as ”nuclei” based on their distinct cyto- and myeloarchitectural characteristics.[1] Current literature shows that different intrathalamic nuclei are part of different cortical relay networks, and regional thalamic changes could account for specific symptoms in different neurological disorders, such as Parkinson’s disease, essential tremor, Alzheimer’s disease, and multiple sclerosis. Surgical methods like Deep Brain Stimulation (DBS) are used to target specific thalamic nuclei and counter the symptoms of neuropsychiatric and movement disorders.[2, 3] Localizing the individual nuclei would thus help in tracking disease progression and intelligent targeting for treatment.

Identification of the intrathalamic nuclei, however, is extremely challenging because clinical T1 or T2 weighted magnetic resonance (MR) images do not present sufficient intrathalamic contrast. Liu et al[4] proposed a scheme to segment a set of 23 nuclei on clinical T1-w MR images using a hierarchical active shape model. The training library for the active shape model was generated by careful expert delineation on multiple high field 7 Tesla (7T) MR sequences on 9 healthy volunteers and was guided by the Morel stereotactic atlas.[1] Although creating the model requires high field 7T MRI, the segmentation algorithm can be applied to clinical 3 Tesla (3T) MR data. Liu et al cross-validated this model on a leave-one-out basis over the 9 subject brains and showed that the shape model method provides higher segmentation accuracy when compared against single-atlas and multi-atlas approaches, with dice values ranging from 0.53 to 0.9 for all nuclei. However, the model only captures the statistical characteristics of a limited sample size, and it is yet to be validated on a larger population. Moreover, the high field MR imaging technique used to generate the library of manually segmented nuclei is not in clinical use, and thus cannot serve as a ground truth for studies performed using clinical MRI scanners. In this paper, we aim to verify and validate the performance of the model in a larger population where only clinical 3T MR data was available.

In particular, we aim to validate the segmentation of the pulvinar nucleus, which is one of the largest thalamic nuclei located at the posterior end of the thalamus and one of the higher-order thalamic relays.[5] Research suggests that it plays a strong role in the brain’s attention networks.[6–10] For example, multiple studies have linked it to the control of visual attentional selection and regulating cortical synchrony,[10–15] and is known to be involved in temporal lobe epileptic seizures.[16, 17] It has been at the forefront of a large body of research on neurodegenerative diseases and segmenting it accurately is important to support these studies. This is challenging because there is no in vivo subject specific gold standard data for any intrathalamic nucleus. Previous studies have shown that there is a strong structural connectivity between the pulvinar and the hippocampus in humans.[18–21] Based on this concept, we propose to use structural connectivity between the hippocampus and the thalamus to validate our segmentation method. Using diffusion tensor images (DTIs)

acquired with a 3T scanner, we created connectivity maps and compared them to our segmentation results.

2. METHODS

Forty-three healthy volunteers were recruited for this study (age 39 ± 13 years, 21 females, 22 males). Clinical T1-weighted three-dimensional MRI and DTI images were acquired using a Philips Achieva 3T MRI scanner (Philips Healthcare, Best, The Netherlands) with a 32-channel head coil. The specifications of the scans are (1) T1-w MRI: gradient echo, repetition time = 9.1 msec, echo time = 4.6 msec, 192 shots, flip angle = 8°, matrix = 256 × 256, 1 × 1 × 1 mm^3 (2) diffusion weighted MRI: b = 1600 s/mm^2, 92 directions, 2.5 × 2.5 × 2.5 mm^3, 1 average. Informed consent was obtained from each subject prior to scanning in accordance with Vanderbilt University Institutional Review Board guidelines.

A thalamus mask, which is required for Liu's method, was segmented in each T1-w MR image using a multiatlas-based segmentation method.[22] The shape model library of Liu et al[4] is defined on a 7T MR atlas and requires a known correspondence between this atlas and the subject T1 image. All subjects were registered to this atlas using a combination of rigid[23] and nonrigid registration,[24] and the 23 distinct nuclei defined in Liu's model were segmented in each hemisphere of each image using the shape model. Because the diffusion images used in the current study have a relatively low resolution, and because DTI-based methods usually can parcellate no more than 14 intra-thalamic structures,[18, 19] the 23 nuclei from the shape model were regrouped into 13 larger subgroups of nuclei, of which S11 is the pulvinar complex of interest (see Table 1 and Figure 1).

We processed the DTI data and performed probabilistic tractography[25] using FMRIB's (Oxford Centre for Functional MRI of the Brain) FSL software (www.fmrib.ox.ac.uk/fsl). The thalamus and hippocampus masks were obtained using FreeSurfer,[26] and were used as the seed and the target respectively to generate the DTI connectivity maps. The analysis was performed separately for each hemisphere. The value of each voxel in these statistical maps represent the number of successful seed-to-target connections out of 5000 trials between the thalamus and the ipsilateral hippocampus, thereby measuring the probabilistic connectivity of each voxel. Distance correction was used to weigh the tracking as the distance from the seed. A population probability map was generated for each hemisphere from the 43 individual maps using age as a covariate using the SPM8 toolbox (http://www.fil.ion.ucl.ac.uk/spm/software/spm8/).

It is known that parts of the anterior thalamus are highly connected to the hippocampus,[27] particularly through the Papez circuit, which could act as a confound when estimating the connectivity of the pulvinar. Therefore, we defined a region of interest (ROI) around the posterior half of the thalamus in the connectivity maps of each subject. The mean connectivity values were determined for all 13 structures wholly or partially included in the ROI, which were then further normalized by the mean value over the entire ROI. The result was a normalized mean connectivity value for each of the 13 subgroups. We used a one-way ANOVA and pairwise comparisons to assess the differences in mean connectivity across the 13 structures. All calculations were carried out in MATLAB (Mathworks, Natick, MA).

3. RESULTS

Our aim was to verify that the pulvinar generated by our segmentation technique (S11 from Table 1) encompasses the strongly connected pulvinar region identified with probabilistic tractography. Boxplots of the normalized mean connectivity values for both the left and the right thalamus are shown in Figures 2a and 2b. A one-way ANOVA between the values obtained over the population between 13 anatomical structures in both hemispheres followed by pairwise comparisons of means revealed that the pulvinar complex has significantly greater ($p < 0.01$) mean connectivity values compared to the other 12 nuclei within this ROI. In fact, the weighted centroid of the connectivity values, defined over the same ROI in each subject's map, was consistently localized (in 42 out of 43 subjects) within the S11 complex. This suggests that the anatomical segmentation correctly identifies the pulvinar region, as shown on the population map in Figure 3 i.e., the anatomical structure S11 encompasses the pulvinar identified from hippocampal connectivity, which validates that the shape segmentation is correctly localized and not overtly conservative.

This analysis can be extended to the 4 nuclei which constitute the S11 complex, while acknowledging the limitations due to resolution. Normalized mean boxplots for the 4 subnuclei in both the left and the right hemispheres are presented in Figures 2c and 2d. A19 is the largest of the 4 subnuclei and cover the medial and inferior parts of the pulvinar, and this is perceptibly more connected to the hippocampus than the other three nuclei. Existing literature suggests that it is the medial part of the pulvinar that is most strongly connected[20] to the hippocampus within the entire pulvinar. Our results agree with this finding, which is a further indication that our segmentation method is not only capable of localizing the pulvinar, but also its medial part in A19.

4. CONCLUSIONS

In this paper, we propose a method for the validation of a statistical shape model-based method designed to segment intrathalamic nuclei, and we apply it to the pulvinar complex of the thalamus. This is challenging due to the low intrathalamic contrast in clinically available MR data and the lack of subject-specific gold standard. Using known patterns of white matter connectivity between the pulvinar and the ipsilateral hippocampus determined by probabilistic tractography, we have verified that our method can localize the pulvinar in a population of 43 healthy subjects. Additionally, the medial and inferior parts of the pulvinar are shown to have the highest mean connectivity, which is consistent with the findings reported in the literature. The method we propose can be extended to other nuclei that are known to be connected to specific brain regions. A straightforward extension that we are currently pursuing is the anterior nucleus of the thalamus, which is known to have strong white matter connections to the hippocampus. But the process is clearly not limited to connectivity between the thalamus and the hippocampus, and can be extended to other cortical regions as well. One limitation of our approach is that it is unable to define the exact outer boundaries of the pulvinar nuclei, which would require relying on other sources of information that would permit localizing adjacent structures like the medial, central, intralaminar, ventral and lateral nuclei.

Finally, both the shape model training and the validation presented in this paper have been carried out exclusively on healthy subjects. One of the major anticipated uses of intrathalamic nuclei segmentation is in neurosurgical planning and investigation of regional changes in neurological disorder. Thus, future work will include verifying that our segmentation method generalizes to patient populations. Overall, developing a robust and generalizable method for segmenting the thalamic nuclei would be valuable for surgical treatment methods, and proper anatomical and structural validation is an important step forward in that direction.

Acknowledgments

This research has been supported by the grants R01NS095291 and R01NS75270 from the National Institute of Neurological Disorders and Stroke. The content is solely the responsibility of the authors and does not necessarily represent the official views of this institute.

References

1. Morel A, Magnin M, Jeanmonod D. Multiarchitectonic and stereotactic atlas of the human thalamus. Journal of Comparative Neurology. 1997; 387(4):588–630. [PubMed: 9373015]
2. Benabid AL, Pollak P, Gao D, Hoffmann D, Limousin P, Gay E, Payen I, Benazzouz A. Chronic electrical stimulation of the ventralis intermedius nucleus of the thalamus as a treatment of movement disorders. Journal of neurosurgery. 1996; 84(2):203–214. [PubMed: 8592222]
3. Chopra A, Klassen BT, Stead M. Current clinical application of deep-brain stimulation for essential tremor. Neuropsychiatric disease and treatment. 2013; 9:1859. [PubMed: 24324335]
4. Liu Y, D'Haese P-F, Newton AT, Dawant BM. SPIE Medical Imaging. International Society for Optics and Photonics; 2015. Thalamic nuclei segmentation in clinical 3t t1-weighted images using high-resolution 7t shape models; 94150E–94150E.
5. Sherman SM, Guillery R. The role of the thalamus in the flow of information to the cortex. Philosophical Transactions of the Royal Society of London B: Biological Sciences. 2002; 357(1428):1695–1708. [PubMed: 12626004]
6. Bender D, Youakim M. Effect of attentive flxation in macaque thalamus and cortex. Journal of neurophysiology. 2001; 85(1):219–234. [PubMed: 11152722]
7. Snow JC, Allen HA, Rafal RD, Humphreys GW. Impaired attentional selection following lesions to human pulvinar: evidence for homology between human and monkey. Proceedings of the National Academy of Sciences. 2009; 106(10):4054–4059.
8. Desimone R, Wessinger M, Thomas L, Schneider W. Cold Spring Harbor symposia on quantitative biology. Vol. 55. International Society for Optics and Photonics; 1990. Attentional control of visual perception: cortical and subcortical mechanisms; 963–971.
9. LaBerge D, Buchsbaum MS. Positron emission tomographic measurements of pulvinar activity during an attention task. Journal of neuroscience. 1990; 10(2):613–619. [PubMed: 2303863]
10. Robinson DL, Petersen SE. The pulvinar and visual salience. Trends in neurosciences. 1992; 15(4): 127–132. [PubMed: 1374970]
11. Strumpf H, Mangun GR, Boehler CN, Stoppel C, Schoenfeld MA, Heinze H-J, Hopf J-M. The role of the pulvinar in distractor processing and visual search. Human brain mapping. 2013; 34(5): 1115–1132. [PubMed: 22488931]
12. Kastner S, Pinsk MA. Visual attention as a multilevel selection process. Cognitive, Affective, & Behavioral Neuroscience. 2004; 4(4):483–500.
13. Olshausen BA, Anderson CH, Van Essen DC. A neurobiological model of visual attention and invariant pattern recognition based on dynamic routing of information. Journal of Neuroscience. 1993; 13(11):4700–4719. [PubMed: 8229193]
14. Shipp S. The brain circuitry of attention. Trends in cognitive sciences. 2004; 8(5):223–230. [PubMed: 15120681]

15. Saalmann YB, Kastner S. Cognitive and perceptual functions of the visual thalamus. Neuron. 2011; 71(2):209–223. [PubMed: 21791281]
16. Guye M, Régis J, Tamura M, Wendling F, Gonigal AM, Chauvel P, Bartolomei F. The role of corticothalamic coupling in human temporal lobe epilepsy. Brain. 2006; 129(7):1917–1928. [PubMed: 16760199]
17. Rosenberg DS, Mauguière F, Demarquay G, Ryvlin P, Isnard J, Fischer C, Guénot M, Magnin M. Involvement of medial pulvinar thalamic nucleus in human temporal lobe seizures. Epilepsia. 2006; 47(1):98–107. [PubMed: 16417537]
18. Behrens T, Johansen-Berg H, Woolrich M, Smith S, Wheeler-Kingshott C, Boulby P, Barker G, Sillery E, Sheehan K, Ciccarelli O, et al. Non-invasive mapping of connections between human thalamus and cortex using diffusion imaging. Nature neuroscience. 2003; 6(7):750–757. [PubMed: 12808459]
19. Johansen-Berg H, Behrens TE, Sillery E, Ciccarelli O, Thompson AJ, Smith SM, Matthews PM. Functional-anatomical validation and individual variation of diffusion tractography-based segmentation of the human thalamus. Cerebral cortex. 2004; 15(1):31–39. [PubMed: 15238447]
20. Barron DS, Tandon N, Lancaster JL, Fox PT. Thalamic structural connectivity in medial temporal lobe epilepsy. Epilepsia. 2014; 55(6)
21. Keller SS, O'muircheartaigh J, Traynor C, Towgood K, Barker GJ, Richardson MP. Thalamotemporal impairment in temporal lobe epilepsy: a combined mri analysis of structure, integrity, and connectivity. Epilepsia. 2014; 55(2):306–315. [PubMed: 24447099]
22. Asman AJ, Landman BA. Non-local statistical label fusion for multi-atlas segmentation. Medical image analysis. 2013; 17(2):194–208. [PubMed: 23265798]
23. Maes F, Collignon A, Vandermeulen D, Marchal G, Suetens P. Multimodality image registration by maximization of mutual information. IEEE transactions on medical imaging. 1997; 16(2):187–198. [PubMed: 9101328]
24. Rohde GK, Aldroubi A, Dawant BM. The adaptive bases algorithm for intensity-based nonrigid image registration. IEEE transactions on medical imaging. 2003; 22(11):1470–1479. [PubMed: 14606680]
25. Behrens TE, Berg HJ, Jbabdi S, Rushworth MF, Woolrich MW. Probabilistic diffusion tractography with multiple fibre orientations: What can we gain? Neuroimage. 2007; 34(1):144–155. [PubMed: 17070705]
26. Fischl B. Freesurfer. Neuroimage. 2012; 62(2):774–781. [PubMed: 22248573]
27. Jankowski MM, Ronnqvist KC, Tsanov M, Vann SD, Wright NF, Erichsen JT, Aggleton JP, O'Mara SM. The anterior thalamus provides a subcortical circuit supporting memory and spatial navigation. Frontiers in systems neuroscience. 2013; 7

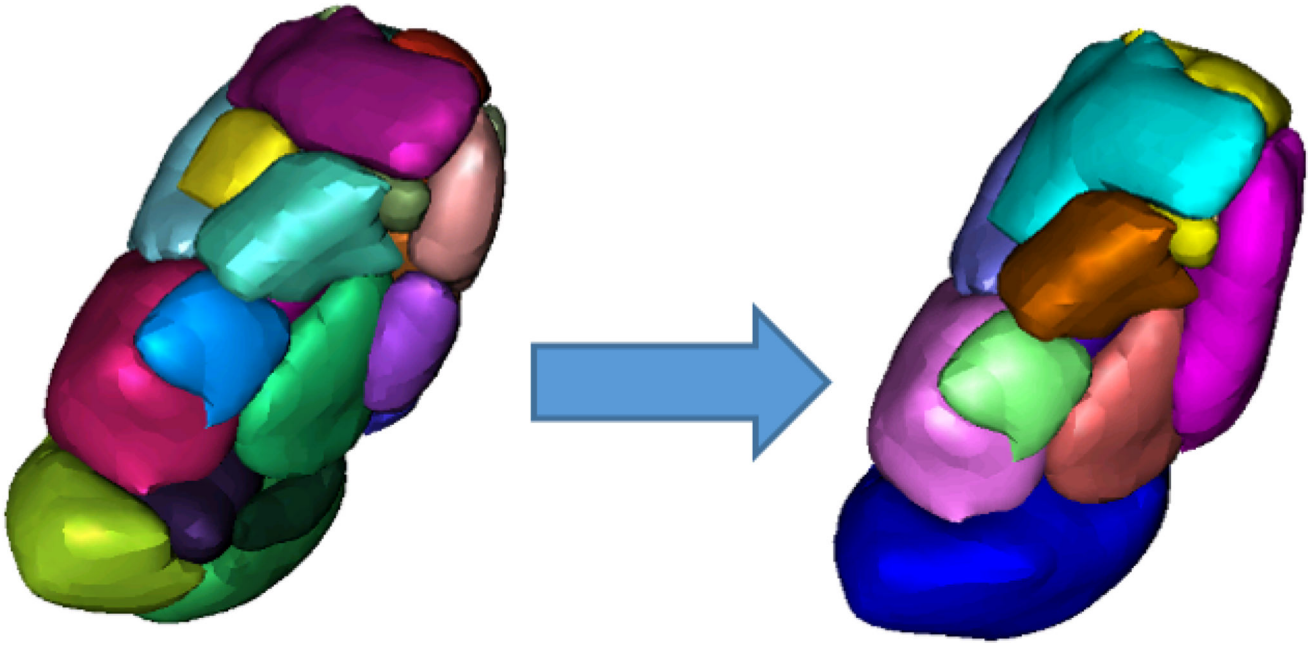

Figure 1.
Original 23 segmented nuclei on the left, regrouped to 13 on the right. Colors do not correspond across figures, but are only used to denote distinct nuclei.

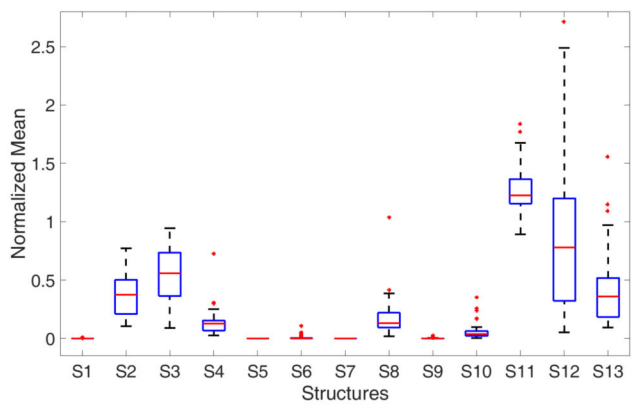

(a) Normalized Mean Connectivity values across 13 structures on the left hemisphere

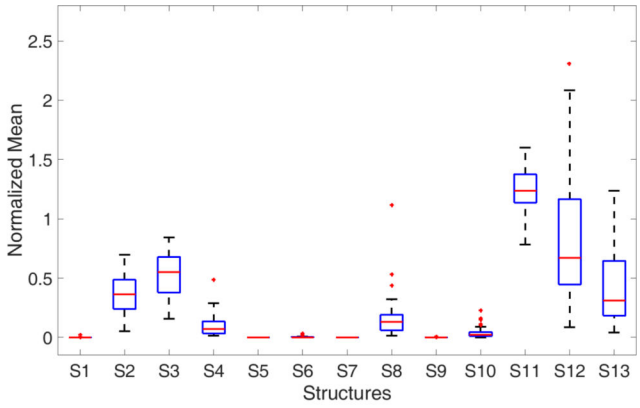

(b) Normalized Mean Connectivity values across 13 structures on the left hemisphere

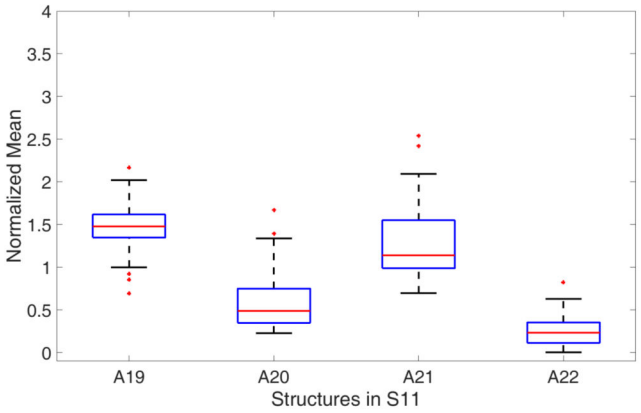

(c) Normalized Mean Connectivity values across 4 nuclei of S11 on the left hemisphere

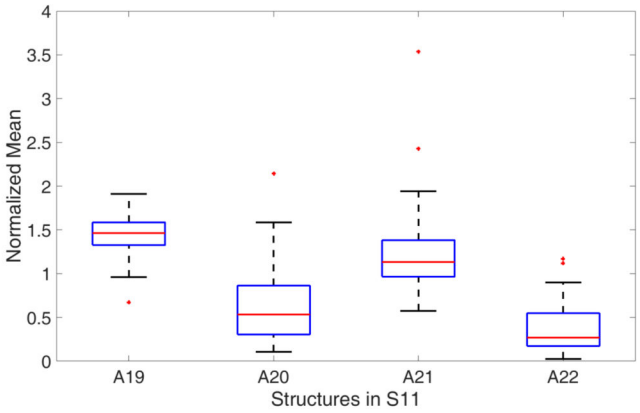

(d) Normalized Mean Connectivity values across 4 nuclei of S11 on the right hemisphere

Figure 2.
Boxplots of the normalized mean connectivity values in different structures.

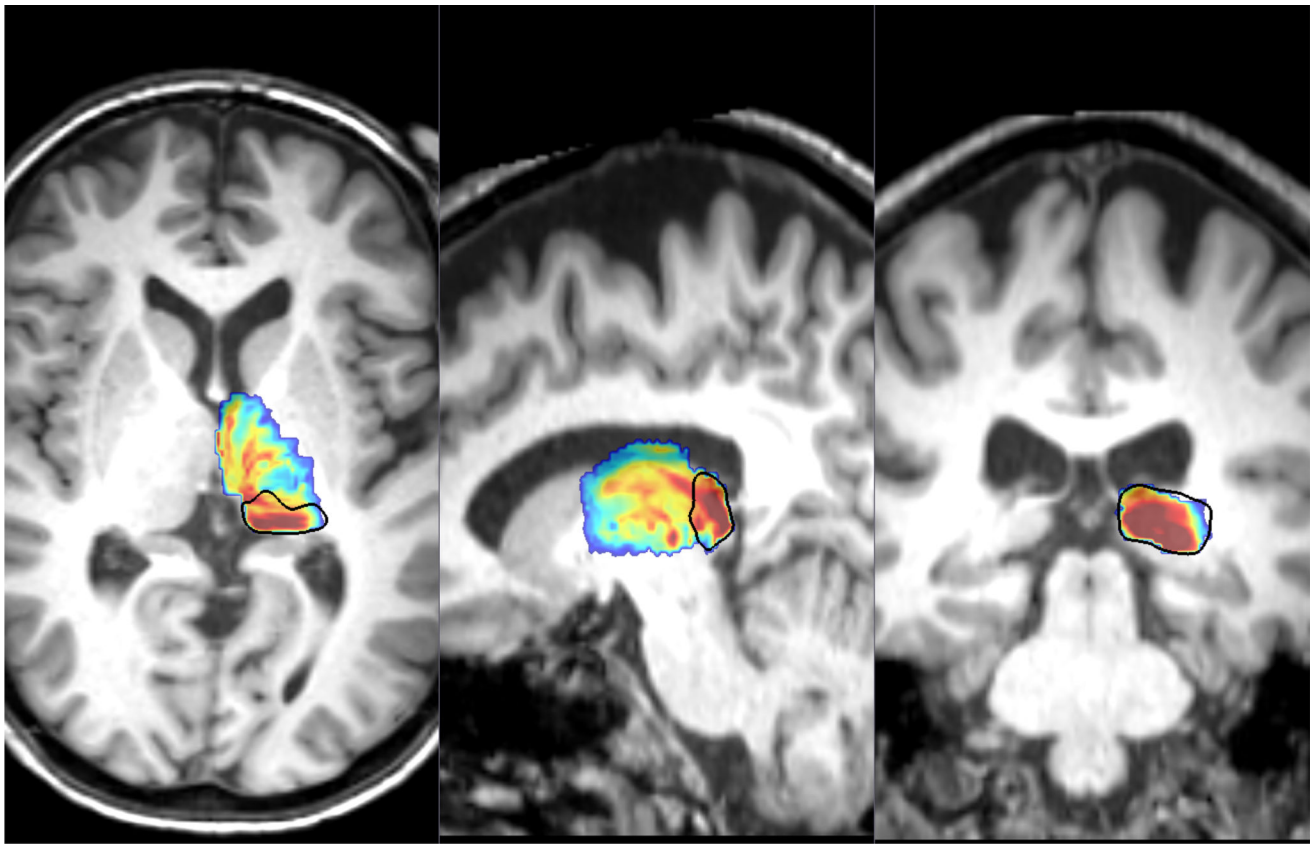

Figure 3.
Segmented Pulvinar (black contour) encompasses highly connected regions of the pulvinar in the population map.

Table 1

Nuclei regrouping and original component nuclei based on the Morel atlas

Regrouped Nuclei	Original Component Nuclei
Anterior (S1)	Anteroventral (A1), Anteromedial (A2), Mammillothalamic tract (A4)
Medial (S2)	Mediodorsal (A5), Parafascicular (A7), Central medial (A9), Paraventricular (A10), Habenular (A11)
Central (S3)	Central lateral (A8)
Intralaminar (S4)	Centre mdian (A6)
Ventral Anterior (S5)	Ventral anterior (A12), Ventral lateral anterior (A13)
Ventral Lateral (S6)	Ventral lateral posterior (A14)
Ventral Medial (S7)	Ventral medial (A15)
Ventral Posterior Lateral (S8)	Ventral posterior lateral (A16)
Ventral Posterior Medial (S9)	Ventral posterior medial (A17)
Ventral Posterior Inferior (S10)	Ventral posterior inferior (A18)
Pulvinar (S11)	Medial and Inferior pulvinar (A19), Anterior pulvinar (A20), Lateral pulvinar (A21), Limitans (A22)
Lateral Dorsal (S12)	Lateral dorsal (A3)
Lateral Posterior (S13)	Lateral posterior (A23)